A Novel Scatterer Trajectory Association Method Based on Markov Chain Monte Carlo Algorithm

Lei Liu, Feng Zhou
The Ministry Key Laboratory of Electronic Information Countermeasure and Simulation, Xidian University
Xi'an, China
liulei_xidian@163.com, fzhou@mail.xidian.edu.cn

***Abstract*—Precise scatterer trajectory association is the basis of three-dimensional (3D) reconstruction utilizing sequential inverse synthetic aperture radar (ISAR) images. To address the occlusion and trajectory crossing of different scatterers, we propose a novel scatterer trajectory association method based on Markov chain Monte Carlo (MCMC) algorithm. Firstly, we derive the ellipse movement characteristics of each scatterer trajectory under stationary rotation motion model of the observed target. Then, we present a Bayesian model and inference algorithm for the scatterer trajectory association problem. MCMC is applied to estimate the scatterer trajectory matrix. Particularly, we design new prior and likelihood evaluation criteria in MCMC by making use of the elliptical movement characteristics of each scatterer trajectory. Simulation results on simulated data validate the effectiveness of the proposed method.**

Keywords—Inverse synthetic aperture radar (ISAR); Markoc chain Monte Carlo (MCMC); trajectory association; ellipse movement

I. INTRODUCTION

Inverse synthetic aperture radar (ISAR) has been widely applied in military and civil fields thanks to its all-day and all-weather surveillance capability [1]. Based on accurately scaled ISAR image series, the three-dimensional (3D) geometry of the target can be reconstructed by the factorization method [2][3][4]. In this method, accurate scatterer extraction and trajectory association are prerequisites for correct matrix factorization. As for scatterer extraction, the available methods include two-dimensional (2D) estimation of signal parameters via rotational invariance techniques (ESPRIT) [5], root-MUSIC [6] and APES [7] etc., which can achieve good performance in high signal-to-noise ratio (SNR). For extracted scatterers, trajectory association remains a challenging task in radar image processing. In the high-frequency regime, the target consists of dominant scatterers, which rotate around the equivalent rotation center and generate different trajectories in the imaging plane after translational motion compensation [8]. Therefore, the scatterer association problem is similar to the multi-target tracking problem, which has found wide applications in video surveillance, computer vision and signal processing. A Markov chain Monte Carlo (MCMC) data association method is proposed in [9] to solve the multi-targets tracking problem and has shown great performance in high dimensional and complicated problems.

Motivated by the successful application of MCMC in multi-target tracking, this paper presents a Bayesian inference for the scatterer trajectory association problem. New prior and likelihood models are designed according to the anisotropy of scatterers and the moving characteristics of scatterer trajectories in the imaging plane. To avoid complicated derivation and manipulation of the intractable posterior distribution, MCMC method is utilized to sample the posterior distribution. Finally, the scatterer trajectory matrix is obtained to reconstruct the 3D target geometry.

The remainder of this paper is organized as follows. Section II introduces the ISAR imaging model and analyzes the characteristics of scatterer trajectories in the imaging plane. Section III derives the Bayesian inference of scatterer trajectory association problem, then presents the designed prior and likelihood models. The detailed procedure of MCMC algorithm is also described in section III. Section IV shows simulation results to verify the validity of the proposed method and Section V concludes the paper.

II. IMAGING GEOMETRY AND SIGNAL MODEL

After translational motion compensation, the 3D imaging geometry of ISAR target observation becomes an equivalent turntable model shown in Fig. 1 of [4]. In the Cartesian coordinate system, the equivalent target rotation center is the origin O. We assume that in the imaging interval, the observed target has constant rotation vector along the OZ axis with modulus to be ω. The radar line of sight (LOS) is along the line between the radar and the rotation center, whose pitch and azimuth angles are φ_l and θ_l, respectively. In the high-frequency regime, the target can be seen as consisting of several isolated scatterers. For an arbitrary scatterer k whose initial position is $\mathbf{p}_0^k = \begin{bmatrix} x_0^k & y_0^k & z_0^k \end{bmatrix}^T$, its new position vector $\mathbf{p}_t^k = \begin{bmatrix} x_t^k & y_t^k & z_t^k \end{bmatrix}^T$ at t can be expressed as

$$\mathbf{p}_t^k = \mathbf{T}_t \mathbf{p}_0^k \tag{1}$$

according to the turntable model described by Fig. 1, where $\mathbf{T}_t$ is the basic rotation transformation matrix, i.e.

$$\mathbf{T}_t = \begin{bmatrix} \cos(\omega t) & -\sin(\omega t) & 0 \\ \sin(\omega t) & \cos(\omega t) & 0 \\ 0 & 0 & 1 \end{bmatrix} \tag{2}$$

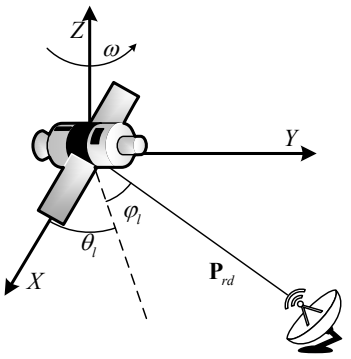

Fig. 1 ISAR imaging geometry

In the equation above, the instantaneous rotational angle of scatterer k is ωt. Suppose the range between radar and the equivalent rotational center is r_0, then, the radar position vector is $\mathbf{p}_{rd}=\left[r_0\cos\varphi_l\cos\theta_l \quad r_0\cos\varphi_l\sin\theta_l \quad r_0\sin\varphi_l\right]^T$ as shown in Fig. 1, and the instantaneous range between the radar and scatterer k is

$$R_t^k \approx r_0-\vec{\mathbf{p}}_{rd}^T\mathbf{p}_t^k=r_0-\vec{\mathbf{p}}_{rd}^T\mathbf{T}_t\mathbf{p}_0^k \tag{3}$$

where $\vec{\mathbf{p}}_{rd}$ is the unit vector of radar LOS and 'T' is the matrix transpose. After performing translational motion compensation and the Fourier transform, we obtain 2D high-resolution ISAR image sequence of the target. At t, the position vector of scatterer k in the imaging plane, i.e. $\mathbf{D}_t^k=\left[u_t^k \quad v_t^k\right]^T$, is computed by

$$\begin{cases} u_t^k=\dfrac{1}{\omega\cos\varphi_l}\cdot\dfrac{\partial\left(r_0-\vec{\mathbf{p}}_{rd}^T\mathbf{T}_t\mathbf{p}_0^k\right)}{\partial t} \\ v_t^k=-\vec{\mathbf{p}}_{rd}^T\mathbf{T}_t\mathbf{p}_0^k \end{cases} \tag{4}$$

where u_t^k and v_t^k denote the cross-range and range positions, respectively. Because the angle between the radar LOS and OZ is $90^\circ-\varphi_l$, the effective rotation angular velocity is $\omega\cos\varphi_l$ [4]. The constant r_0 is omitted when computing the range position. Substituting $\vec{\mathbf{p}}_{rd}$, $\mathbf{T}_t$ and $\mathbf{p}_0^k$ into Eq. (4), the 2D projection positions of scatterer k on the imaging plane can be expressed as follows

$$\begin{cases} u_t^k=\begin{bmatrix}\sin\left(\omega t-\theta_l\right)\\ \cos\left(\omega t-\theta_l\right)\end{bmatrix}^T\begin{bmatrix}x_0^k\\ y_0^k\end{bmatrix} \\ v_t^k=\begin{bmatrix}-\cos\varphi_l\cos\left(\omega t-\theta_l\right)\\ \cos\varphi_l\sin\left(\omega t-\theta_l\right)\end{bmatrix}^T\begin{bmatrix}x_0^k\\ y_0^k\end{bmatrix}-z_0^k\sin\varphi_l \end{cases} \tag{5}$$

During the rotation around the OZ axis, the scatterer has constant z_0^k and r_k, where r_k is the radius of scatterer k in the cylindrical coordinate system and can be calculated by $r_k=\sqrt{\left(x_0^k\right)^2+\left(y_0^k\right)^2}$. Therefore, the trajectory of scatterer k in the imaging plane is an ellipse described by the equation below,

$$\frac{\left(u_t^k\right)^2}{r_k^2}+\frac{\left(v_t^k+z_0^k\sin\varphi_l\right)^2}{\left(r_k\cos\varphi_l\right)^2}=1 \tag{6}$$

Eq. (6) indicates that the ellipse center is $\left[0,-z_0^k\sin\varphi_l\right]$, and the major and minor axes are r_k and $r_k\cos\varphi_l$, respectively. Since the assumption of ideal turntable imaging model, the pitch angle φ_l of radar LOS is thought as a constant. Therefore, the trajectory of scatterer k is indeed an ellipse. To generate the image sequence, we first divide the wide angle echoes of the observed target into overlapping sub-apertures, and then process each sub-aperture successively. Then, the number and projected positions can be extracted using 2D ESPRIT, of which the detailed procedure can be found in [5].

III. MCMC BASED SCATTERER TRAJECTORY ASSOCIATION METHOD

A. Bayesian Inference for Scatterer Trajectory Association Problem

Due to the anisotropy of scattering coefficients, scatterers cannot be always detected and extracted at entire observation interval. Hence, we assume that the scattering coefficient of scatterer k is below the detection threshold of 2D ESPRIT except in the interval $\left\{t_s^k,t_e^k\right\}$. Therefore, in scatterer trajectory association problem, what we want to solve is the scatterer number K, the existing interval $\left\{t_s^k,t_e^k\right\}$ and the trajectory of each scatterer.

Let $W_t=\left\{\mathbf{w}_t^n:n=1,\cdots,n_t\right\}$ and n_t be the position set and the number of extracted scatterers at instant t, $W=\left\{W_t:1\le t\le T\right\}$ the set of all the extracted scatterers in the entire observation interval. T denotes the observation interval. Let Ω be the set of all the possible scatterer association states, we have $\varpi\in\Omega$ with ϖ satisfying the following restrictions [9]:

(1) $\varpi=\left\{\beta_0,\beta_1,\ldots,\beta_K\right\}$;

(2) $\bigcup_{k=0}^{K}\beta_k=W$ and for any $i\ne j$, $\beta_i\cap\beta_j=\varnothing$;

(3) β_0 is the set of all false alarm points;

(4) For any $k=1,\ldots,K$ and $t=t_s^k,t_s^k+1,\ldots,t_e^k$, $\left|\beta_k\cap W_t\right|=1$;

(5) For any $k=1,\ldots,K$, $\left|\beta_k\right|\ge 2$ holds;

The restrictions above define the transformation model of scatterer association state. In constraint (1), all the extracted scatterers are divided into $K+1$ sets with K scatterer trajectory sets and one false alarm set. Constraint (2) means

that one extracted scatterer can only belong to one set. Constraint (4) shows that each scatterer corresponds to at most one extracted point at each instant. Since we extract the scatterers using 2D ESPRIT according to their amplitudes, the detection probability of each scatterer is set to be one in the existing interval. Therefore, each scatterer trajectory set will definitely have intersection with W_t in its existing interval $\left\{t_s^k, t_e^k\right\}$. According to constraint 5), the trajectory of each scatterer must have no less than two extracted points to make it distinguishable from the false alarm point.

Therefore, what scatterer trajectory association does is to estimate the partition set ϖ with maximum a posterior given the extracted scatterer set W. According to the Bayes rule, the posterior $p(\varpi \mid W)$ can be expressed as follows

$$p(\varpi \mid W) = \frac{p(W \mid \varpi)\, p(\varpi)}{\sum_{\varpi} p(W \mid \varpi)\, p(\varpi)} \tag{7}$$

where $p(\varpi)$ and $p(W \mid \varpi)$ represent the prior and likelihood. Since it is hard to enumerate all possible sets of ϖ, we cannot compute the value of $\sum_{\varpi} p(W \mid \varpi)\, p(\varpi)$ analytically. To obtain the right scatterer trajectory association, we will therefore use an MCMC sampling method. Before presenting the algorithm, we first construct the prior and likelihood models considering the characteristics of scattering coefficients and scatterer trajectory.

B. Prior Modeling

In ISAR imaging, the movements of different scatterers can be viewed as independent. Each scatterer can be detected and extracted in a specific interval $\left\{t_s^k, t_e^k\right\}$. The prior of ϖ should define the probability model of appearance, disappearance, detection and false alarm. An integrated scatterer trajectory can be interpreted as two or more separated trajectories, which means increasing number of newly appearing and disappearing scatterers at different instants. Actually, we hope that associated scatterer trajectories have longer existing intervals and lower false alarm rate, which facilitates the following 3D reconstruction. Therefore, the smaller the newly appearing scatterer number are, the better the scatterer trajectory association results are. Hence, we model that the number of newly appearing scatterers at each instant has a Poisson distribution with a parameter λ_b, and each scatterer disappears at different instants with probability p_z. The larger the probability of scatterers appearing and disappearing at the observation interval is, the better the integrity of scatterer trajectories are.

Let e_{t-1} be the number of associated scatterers at $t-1$, z_t be the number of disappeared scatterers at t, and a_t be the number of newly appeared scatterers at t. Then, the number of existing scatterers at t is $e_t = e_{t-1} - z_t + a_t$. As the detection probability is set to be 1, the number of detected scatterers d_t is equal to e_t. Therefore, $f_t = n_t - d_t$ is the number of false alarm points at t, which is modeled as appearing with probability p_f. Given the set W of extracted scatterers, the prior of ϖ is modeled by

$$P(\varpi) \propto \prod_{t=1}^{T} p(a_t \mid \lambda_b)\, p_z^{z_t} \left(1-p_z\right)^{e_{t-1}-z_t}\, p_f^{f_t} \left(1-p_f\right)^{d_t} \tag{8}$$

where $p(a_t \mid \lambda_b) = \lambda_b^{a_t} e^{-a_t} / a_t!$ denotes the probability density of newly appearing scatterers at instant t.

C. Likelihood Modeling

The likelihood evaluates the probability of the scatterer association state. According to section II, the projection of the scatterer trajectory in the imaging plane is an ellipse, whose origin, major axis, and minor axis are functions of the target size and the slowly changing pitch angle. For the correctly associated scatterer, its trajectory forms an ellipse and thus has the minimum root mean square error (RMSE) in ellipse curve fitting [10]. For incorrect scatterer association, the curve fitting generates a large RMSE. For the associated trajectory of *kth* scatterer, let the RMSE of curve fitting be δ_k, the range shift vector of adjacent scatterers be α_k, and the direction vector of adjacent scatterer be β_k at each association state. Then, the likelihood is expressed as follows

$$P(W \mid \varpi) \propto \exp\left\{-\Lambda_1\left[\mathrm{aver}\left(\delta + \Lambda_2 \cdot \varepsilon\right) + \max\left(\delta + \Lambda_2 \cdot \varepsilon\right)\right]\right\} \tag{9}$$

with

$$\varepsilon_k = \mathrm{std}\left(\alpha_k\right) \cdot \mathrm{std}\left(\mathrm{diff}\left(\beta_k\right)\right) \tag{10}$$

In (9) and (10), $\mathrm{aver}(\cdot)$ denotes the average, $\mathrm{std}(\cdot)$ the standard deviation, and $\mathrm{diff}(\cdot)$ the differential vector. $\delta = [\delta_2, \delta_3, \cdots, \delta_K]$ is the vector of RMSE in ellipse curve fitting; and $\varepsilon = [\varepsilon_2, \varepsilon_3, \cdots, \varepsilon_K]$ evaluates the continuity and stability of associated trajectories.

D. Markov Chain Monte Carlo Method

We have defined the prior $p(\varpi)$ and likelihood $p(\varpi \mid W)$ given the extracted scatterer set W. To obtain the scatterer trajectories, we propose utilizing MCMC for parameter estimation. MCMC is widely used to approximate integrals over complex probability distributions. By constituting one Markov chain M with the state space Ω and the stationary distribution $\pi(\varpi)$, MCMC generates one new sample from $\pi(\varpi)$ based on a proposal distribution and then decides whether or not to accept the new sample.

One widely used MCMC method is the Metropolis-Hastings (M-H) algorithm [11]. If the current state of the Markov chain is $\varpi \in \Omega$, then, the new state $\varpi' \in \Omega$ is generated according to the proposal distribution $q(\varpi, \varpi')$, and ϖ' will be accepted with probability $A(\varpi, \varpi')$ given by

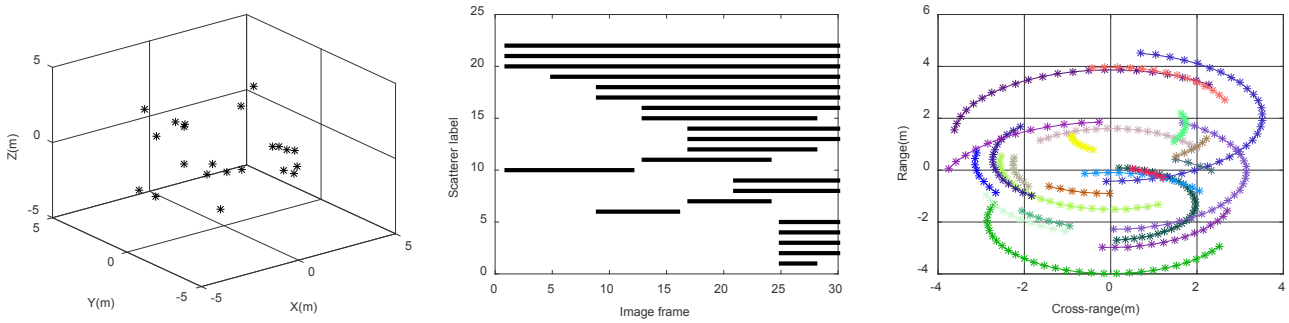

(a) (b) (c)

Fig. 2 (a) Simulated scatterer model and (b) existing intervals of different scatterers and (c) theoretical projection trajectories.

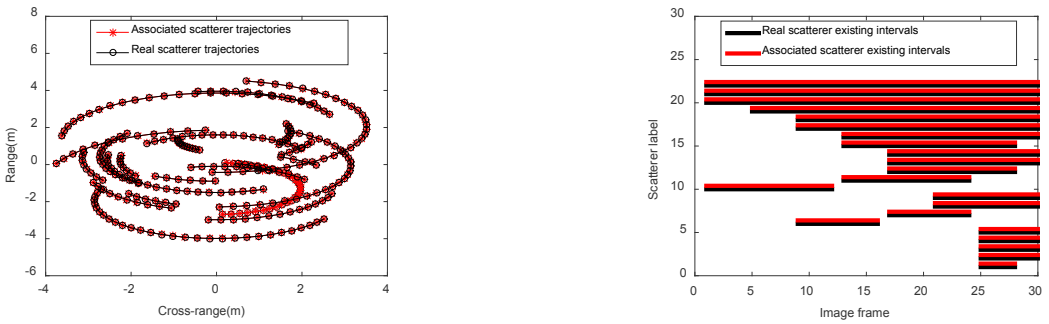

(a) (b)

Fig. 3 (a) Comparison between the real scatterer trajectories and associated scatterer trajectories; (b) comparison between the real scatterer existing intervals and reconstructed scatterer existing intervals.

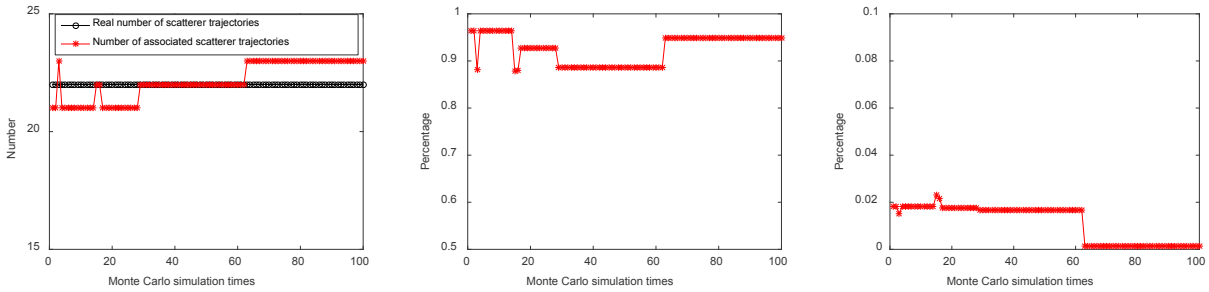

(a) (b) (c)

Fig. 4 Experimental results.(a) comparison between real number of scatterer trajectories and the number of associated scatterer trajectories; (b) average value of $\delta_{R,k}$ in each Monte Carlo simulation; (c) average value of $\delta_{W,k}$ in each Monte Carlo simulation.

$$A(\varpi,\varpi') = \min\left(1, \frac{\pi(\varpi')q(\varpi',\varpi)}{\pi(\varpi)q(\varpi,\varpi')}\right) \tag{11}$$

Ref. [9] defines eight types of proposal distributions, including birth/death, split/merge, extension/reduction, and switch/update. The transition probability $q(\varpi,\varpi')$ or $q(\varpi',\varpi)$ is computed according to the present state ϖ. In the above equation, $\pi(\varpi)$ is the probability of each scatterer association state in the stationary distribution, and is equal to the posterior probability $P(\varpi \mid W)$.

IV. Simulation Results

In this section, several points with random positions and existing intervals are used as the simulated scatterer model, which is shown in Fig. 2 (a). The total number of scatterers is 22. The simulated radar works at X band and the bandwidth of the transmitted signal is 1 GHz. The equivalent rotation angular velocity of the observed target is 0.16rad/s. The total observation interval is 19.2s which contains about 1920 pulses. The wide angle data is divided into adjacent sub-apertures, whose window length and step are both 64. The existing intervals of different scatterers are generated randomly, which are shown in Fig. 2 (b). It shows that different scatterers emerge and disappear at random instants. The theoretical projected trajectories of all the scatterers are presented in Fig. 2 (c), and the ellipse characteristics movement are such obvious.

$$\delta_{R,k} = \frac{Number\ of\ successfully\ associated\ scatterers\ in\ trajectory\ k}{Total\ scatterer\ number\ of\ corresponding\ real\ reajectory} \tag{12}$$

$$\delta_{W,k} = \frac{Number\ of\ wrong\ associated\ scatterers\ in\ trajectory\ k}{Total\ scatterer\ number\ of\ corresponding\ real\ reajectory} \tag{13}$$

After the extraction of scatterers, we obtain the scatterer set of each sub-aperture. MCMC is then applied to associate the scatterers extracted from different sub-apertures. Because different scatterers occupy different existing intervals, the association processing is rather complicated. The maximum number of Monte Carlo iteration is set as 20000 and finally 22 scatterer trajectories are extracted successfully. The scatterer association result is presented in Fig. 3(a), which shows that associated scatterer trajectories match with real scatterer trajectories well. The comparison between real scatterer existing intervals and associated scatterer existing intervals is presented in Fig. 3 (b), which shows that associated scatterer trajectories have the same existing intervals with real scatterer trajectories. Therefore, the effectiveness of the proposed trajectory association method is verified.

To further analyze the performance of our proposed method, 100 independent Monte Carlo simulations are done after extracting the scatterers of each image frame. Here, we utilize two metrics [9] to evaluate the performance of each associated scatterer trajectory as shown in Eq. (12) and (13) where $\delta_{R,k}$ denotes the rate of the number of successfully associated scatterers to the total number of corresponding real scatterer trajectory, $\delta_{W,k}$ represents the rate of the number of wrong associated scatterers to the total number of corresponding real scatterer trajectory. Hence, larger $\delta_{R,k}$ and smaller $\delta_{W,k}$ mean better performance of the proposed method. Fig. 4 (a) shows that the proposed method can associate almost all the scatterer trajectories. Fig. 4 (b) and (c) present the values of $\delta_{R,k}$ and $\delta_{W,k}$ in each Monte Carlo simulation, respectively, which are above 0.85 and below 0.03 in all the Monte Carlo simulations, respectively. Therefore, the effectiveness of the proposed trajectory association algorithm is verified.

V. CONCLUSION

As a crucial step of 3D geometry reconstruction method using ISAR sequential images, a novel scatterer trajectory association method is proposed. Based on the analysis of the movement characteristics of scatterer trajectories, the prior model, likelihood model and posterior model are designed. MCMC is performed to estimate the true scatterer number and the association state, of which the posterior probability is the maximal. The simulation results have proved the effectiveness of the proposed algorithm. However, the scatterers and imaging scenario considered in the simulation are rather ideal. To make the proposed method applicable for the real data, more future work will be done to tackle the sliding scattering centers and complicated target motion. Meanwhile, the associated scatterer trajectory matrix is incomplete when the existing intervals of different scatterers are different. Therefore, traditional factorization method cannot be applied directly. 3D geometry reconstruction algorithm using incomplete scatterer trajectory matrix will be studied in our future research.

ACKNOWLEDGMENT

The authors would gratefully acknowledge the Postdoctoral Science Foundation of China under Grant 2016M602775 and 2017M613076 for funding.

REFERENCES

[1] C. C. Chen, and H. C. Andrews, "Target-motion-induced radar imaging," IEEE Trans. Aerosp. Electron. Syst., vol. 16, no. 1, pp. 2-14, Jan. 1980.

[2] F. E. McFadden, "Three-dimensional reconstruction from ISAR sequences," Proc. SPIE, vol. 4744, pp. 58-67, 2002.

[3] G. Li, J. Zou, and S. Xu, et al., "A method of 3D reconstruction via ISAR sequences based on scattering centers association for space rigid object," Proc. SPIE, vol. 9252, pp. 92520N-1~6, 2014.

[4] L. Liu, F. Zhou, and X. R. Bai, et al., "Joint cross-range scaling and 3D geometry reconstruction of ISAR targets based on factorization method," IEEE Trans. Image Process., vol. 25, no. 4, pp. 1740-1750, Apr. 2016.

[5] R. Roy, and T. Kailath, "ESPRIT-Estimation of signal parameters via rotational invariance techniques," IEEE Tran. Acoust. Speech Signal Proces., vol. 37, no. 7, pp. 948-995, Jul. 1989.

[6] K. M. Cuomo, J. E. Piou, and J. T. Mayhan, "Ultrawide-band coherent processing," IEEE Trans. Antennas Propagat., vol. 47, no. 6, pp. 1094-1107, Jun. 1999.

[7] J. Li, and P. Stoica, "An adaptive filtering approach to spectral estimation and SAR imaging," IEEE Trans. Signal Process., vol. 44, no. 6, pp. 1469-1484, Jun. 1996.

[8] L. Liu, F. Zhou, and M. L. Tao, et al., "Cross-range scaling method of inverse synthetic aperture radar image based on discrete polynomial-phase transform," IET Radar Sonar Navigat., vol. 9, no. 3, pp. 333-341, Mar. 2015.

[9] S. Oh, S. Russell, and S. Sastry, "Markov chain monte carlo data association for multi-target tracking," IEEE Trans. Automat. Control, vol. 54, no. 3, pp. 481-497, Mar. 2009.

[10] A. Fitzgibbon, M. Pilu, and R. B. Fisher, "Direct least square fitting of ellipses," IEEE Trans. Pattern Anal. Mach. Intell., vol. 21, no. 5, pp. 476-480, May 1999.

[11] W. K. Hastings, "Monte Carlo sampling methods using Markov chains and their applications," Biometrika, vol. 57, no. 1, pp. 97-109, Jan. 1970.